Fröhlich Electromagnetic Field Generated by Living Cells: Computer Results

J. POKORNÝ, K. VACEK and J. FIALA
Department of Chemical Physics, Faculty of Mathematics and Physics of Charles University, 121 16 Prague 2, Czechoslovakia

ABSTRACT: The Fröhlich coherent polar vibrations may be a source of the cell-generated electromagnetic field. The cellular membrane is assumed to be the locus of the dipole vibrations. We adopt a model of the spherical dipole layer with both uniform and domain distributions of the dipole densities and of the dipole moments. Computer results indicate that the electromagnetic field of cellular origin may be significant within a distance of about 1 - 10 μm from the cell surface. The Schottky barrier might be used to determine the frequency and the intensity of the cell-generated field in the frequency range below 1 THz.

INTRODUCTION

Coherent vibration states in biological systems were theoretically predicted by Fröhlich (1968a, 1968b). Polarization waves consisting of normal modes are capable of coherent state excitation if the metabolic energy supply exceeds a threshold value, if long-range interaction between vibration systems exists, and if energy is exchanged between particular modes and surroundings. Especially the χ-process of the energy exchange is important (Fröhlich, 1968b, 1977). The lowest frequency mode is always coherently excited with a high energy storage (Fröhlich, 1968a, 1968b, 1972, 1977). Under convenient conditions even the higher-frequency modes may be simultaneously sustained in the coherent states (Pokorny, 1982).

The polar coherent vibrations of the cellular membranes or of the microtrabecular cytoskeleton (Del Giudice, et al., 1982) may be a source of the cell-generated electromagnetic field. The theoretical prodiction estimates the fundamental frequency of the oscillations to be about 0.1 THz for the membrane generation and about 0.1 GHz for the cytoskeleton one. Laser-Raman spectroscopy of living cells of *Bacillus megaterium* and of *Escherichia coli* has revealed a frequency spectrum of oscillations in the frequency range 0.1 - 100 THz (Webb, 1977, 1980). On the basis of microdielectrophoresis (i.e. attraction of small dielectric particles by living cells) the frequency has been assessed to be of the order of 1 - 10 MHz (Pohl, 1980a).

The cell-generated electromagnetic field most likely mediates the long-range selective interaction in biological systems (Fröhlich, 1968b, 1972, 1978), e.g. between cells (Pokorny, 1980). The long-range interaction forces between cells were revealed from cellular collision observations (Rowlands, et al., 1981). The collision frequency of human living erythrocytes differs significantly from the Brownian motion value. On the other hand, such living erythrocytes with metabolic energy supply cut off and with the zeta potential unchanged (e.g. the static membrane potential undisturbed) obey Brownian motion statistics. Further experimental verification of the erythrocyte interactions indicates that the attraction begins to be effective when the cell membranes are 4 μm apart (Rowlands, et al., 1982; Rowlands and Sewchand, 1982; Sewchand, et al., 1982). The attraction depends on the presence of certain long molecules in the suspending medium. The force field outside the cells is an oscillating electric field in nature, as is proved by microdielectrophoresis (Pohl, 1980a, 1980b; Roy, et al., 1981; Pohl, et al., 1981). The number of attracted dielectric particles depends on the permittivity of the particles as well as on the conductivity of the liquid medium around the cells. The electromagnetic field may undergo significant changes during the cell cycle (Pohl, 1981a; Pohl, et al., 1981). A survey of experimental verifications is given by Fröhlich (1980, 1983).

The morphology of living cells is rich. Some cells have a spherical form (e.g., white blood cells, whose diameters are about 10 μm). For the sake of analytical convenience we adopt a spherical model of the cell. Radiation from spherical dipole layers is computed. Theoretical analysis of the cell-generated electromagnetic field is necessary to reveal the principal features of the field, i.e. the frequency and the space dependence of the intensity. This may be valuable for development of appropriate measuring methods.

UNIFORM SPHERICAL DIPOLE LAYER

We assume a spherical dipole layer consisting of identical elementary electric dipoles whose moments and effective cross sections (i.e. the reciprocal values of the number of dipoles per unit area) are P_d and S_d, respectively. The dipole axes are oriented radially. The formulae for the electric field radiated by an electric dipole are given e.g. by Stratton (1941). All the dipole terms (i.e. the terms giving rise to radiation as well as the terms accounting for the energy stored in the near field) are included in the evaluation. Instead of the real permittivity the complex one is used, which holds for the harmonically varying fields in a conductive medium. This partially

covers the effects of conductivity of the liquid medium around the cell on the electric field (but the screening effect of charges at the boundaries of different media is neglected). The values of the relative complex permittivities $\varepsilon_k = \varepsilon' + i\varepsilon''$ are given in Tab. 1. The parameters given in Table 1 are those for water, since the main component of the extracellular liquid is water, which determines the electrical parameters of the extra cellular medium in the frequency range under consideration.

A macroscopic uniform spherical dipole layer with continuous charge distribution does not generate any electromagnetic field when the medium is homogeneous and isotropic regardless of the excitation, i.e. of the energy of dipole oscillations. The membrane dipole layer very likely consists of discrete elementary dipoles as well as of aggregates of elementary dipoles. The dipole moments and dipole space distributions are subjected to fluctuations of thermal origin. Perturbations of the coherent state occur. Interaction between vibrating dipoles mediated by the generated electromagnetic field acts against the fluctuations (due to forced vibrations). This effect is connected with energy losses of the generated electromagnetic field. The energy losses contribute to keeping the coherence of oscillation. The medium inside the cell is inhomogeneous owing to microtrabecular cytoskeleton and cellular organelles. A field around the cell is generated, therefore, even by a uniform spherical dipole layer.

The radial electric field around the model spherical layer is given by the integral

$$\tilde{E}_R = \frac{1}{S_d} \iint_{\partial\delta} (E_r \cos\alpha - \tilde{E}_\partial \sin\alpha)\, R_o^2 \sin\delta \, d\gamma \, d\partial$$

where E_R is the complex intensity of the radial electric field and E_r, E_δ are the complex intensities of the electric field generated by the elementary dipoles along the spherical coordinates r, δ, respectively (Fig. 1). The meaning of all the other symbols in Eq. 1 (i.e. α, γ, δ, R_o) follows from Fig. 1. Numerical integration of Eq. 1 is performed to add the field contributions of the dipoles. The computed curves of the amplitude of the radial electric field intensity versus distance from the cell surface are shown in Fig. 2. The lower set of curves represents the field generated by a spherical layer of uniformly distributed aggregates of dipoles in homogeneous isotropic medium. The centers of identical dipole aggregates are assumed to be 20 nm apart. To simplify the numerical evaluation the aggregates are replaced by equivalent discrete dipoles whose total moments are equal to the sum of all the elementary dipole moments in each aggregate. Numerical integration of Eq. 1 is performed over all the layer. The amplitude E_R depends on all the spherical coordinates. A lobe pattern of the field corresponds to the space distribution of the equivalent dipoles. The E_R values are determined along the radial line in the middle of equivalent dipoles. If part of the generating surface invisible from the point of observation is effectively screened, the intensity of the electric field in a particular direction may be considerably greater than that given by the lower set of curves in Fig. 2. The upper set of curves represents the generation from a part of the spherical surface visible from the point of observation. The curves may be assumed as a certain upper limit of the amplitude E_R along the lobe axis. The real generated field curves might be expected to lie between the two sets of curves in Fig. 2.

TABLE 1
Parameters of water in the frequency range from 1 GHz to 10 THz

	$\tau_f/4$	ε'	ε''	σ	τ	τ'
(GHz)	(s)			(S/m)	(s)	(s)
1	$2.5\ 10^{-10}$	80	5	0.28	$2.5\ 10^{-9}$	$6.9\ 10^{-11}$
3	$8.3\ 10^{-11}$	75	12.5	2.1	$3.2\ 10^{-10}$	$5.5\ 10^{-11}$
10	$2.5\ 10^{-11}$	60	30	16.7	$3.2\ 10^{-11}$	$2.0\ 10^{-11}$
30	$8.3\ 10^{-12}$	25	32	53	$4.1\ 10^{-12}$	$3.5\ 10^{-12}$
60	$4.2\ 10^{-12}$	12.5	20	66.8	$1.7\ 10^{-12}$	$1.4\ 10^{-12}$
100	$2.5\ 10^{-12}$	8.5	12.5	69.5	$1.1\ 10^{-12}$	$9.5\ 10^{-13}$
300	$8.3\ 10^{-13}$	5	5	83.5	$5.3\ 10^{-13}$	$4.7\ 10^{-13}$
1000	$2.5\ 10^{-13}$	4.5	2.5	139	$2.9\ 10^{-13}$	$2.7\ 10^{-13}$
3000	$8.3\ 10^{-14}$	3	1.7	284	$9.4\ 10^{-14}$	$9.0\ 10^{-14}$
10000	$2.5\ 10^{-14}$	2	1	556	$3.2\ 10^{-14}$	$3.1\ 10^{-14}$

The meaning of all the symbols is explained in the text.
Permittivity values after NCRP Rep. 67 (1981).

The computed results indicate the significant values of the electric field intensity within a distance of about 1 - 10 μm from the cell surface.

NONUNIFORM DIPOLE LAYER

The energy supply to the vibration systems, energy losses, and energy channeling between different modes may exhibit significant space dependence. Domain distribution of vibrations on the cellular surface may exist (Pohl, 1980a). The phase and the amplitude of the coherent vibrations as well as the dipole density and the dipole axes orientations may depend on the location of oscillators on the spherical surface. Definite, nonrandom space distribution of all these quantities must exist over the spherical layer to fulfil a general coherence condition. For example, the amplitude of the dipole moments or the dipole density may be greater (or smaller) in particular areas than in the remaining part of the spherical surface. A series of tesseral harmonics functions may be used to describe a nonuniform dipole layer. To express amplitude of the dipole moments we used one of these functions (Stratton, 1941).

$$F = (15/16)\ (3 + 4\ \cos 2\Theta - 7\ \cos 4\Theta)\ \cos\ 2\phi, \quad (2)$$

where Θ, ϕ are the spherical coordinates of the cell.

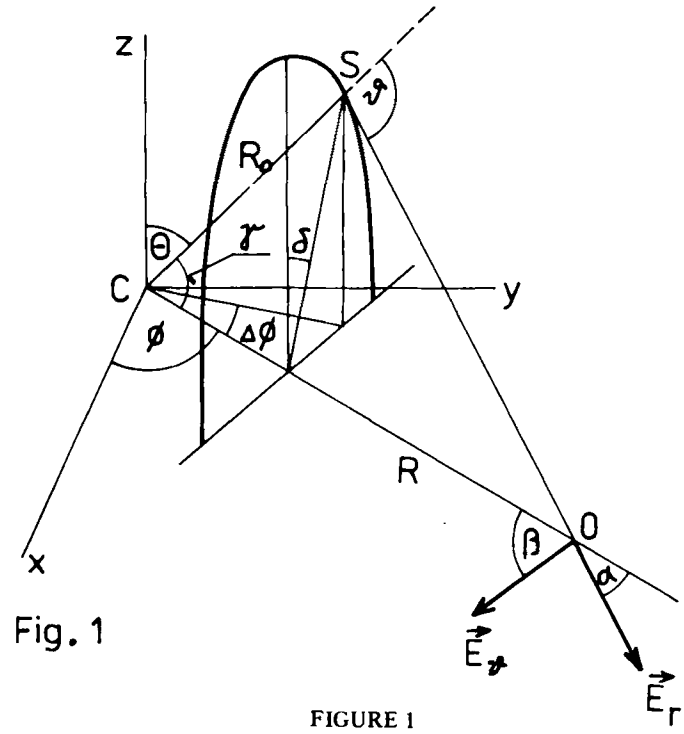


FIGURE 1

Schematic plot of the cross section of the spherical surface generating the electromagentic field. R is perpendicular to the cross section plane. C - center of the sphere, S - point of radiation, O - point of observation. The radius R_o of the spherical layer is 5 μm.

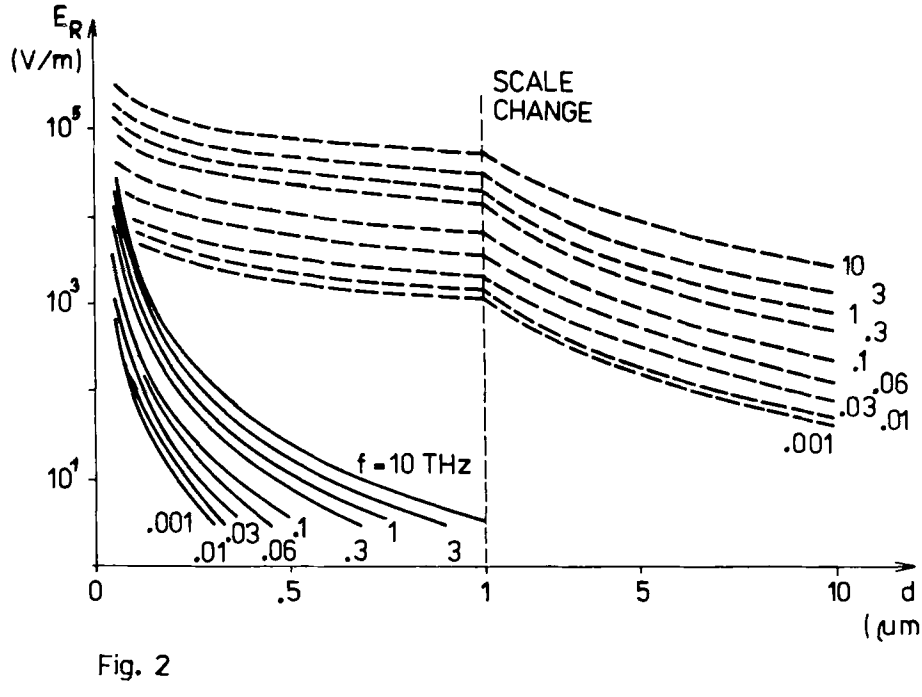


FIGURE 2

The amplitude E_R of the intensity of the electric field versus distance $d = R - R_o$ in the frequency range 0.001 - 10 THz. The field is generated by uniformly distributed aggregates of dipoles about 20 nm apart with a total dipole moment about 4 el, which corresponds to a moment P_{do} = 0.01 el of uniformly distributed dipoles of cross section S_d = 1 nm^2. e is the elementary charge and l is the membrane thickness; we use l = 5 nm. Integration is performed over all the spherical surface (full curves) and over the area visible from the point of observation (dashed curves).

The radial component of the electric field intensity is computed with the aid of Eq. 1. Integration is taken over all the spherical surface. A homogeneous medium is assumed. The dipole moments are $P_{do}F$. The amplitude of the complex intensity E_R as a function of R and ϕ is plotted in Fig. 3. In the vicinity of the generating surface the intensity of the field is about one order greater than that given by the set of dashed curves in Fig. 2. This holds, however, only in particular directions, where the function F given by Eq. 2 acquires its extreme value $|F_m| = 7.5$. The lobe character of the generated field is evident from Fig. 3b, where the $E_r = E_r(\phi)$ dependence is given.

Besides the radial component of the intensity the component directed along the spherical surface is generated. The greatest intensities of the tangential electric field are in the equatorial plane for $\phi = \pm \pi/4$ and $\pm 3\pi/4$. The amplitudes of the intensities are nearly one order smaller than those of the radial components, as follows from computer results.

The forces connected with the tesseral harmonics field might cause ruffling of the cellular membrane.

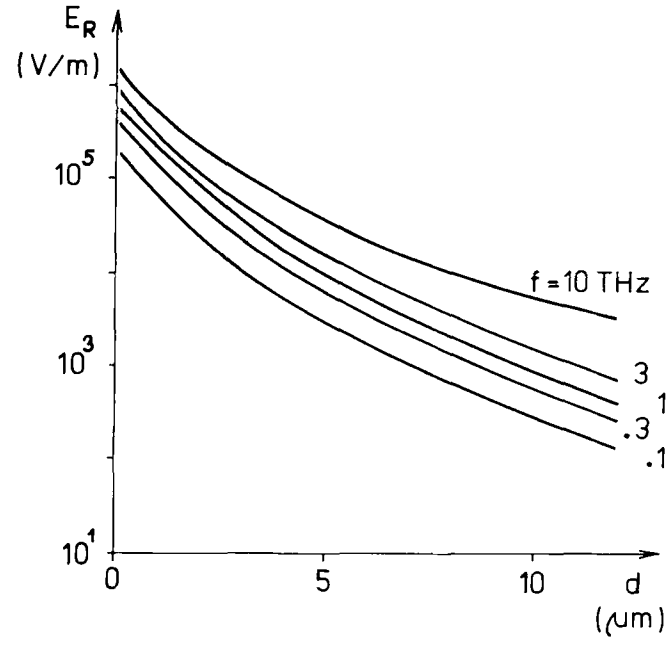


Fig. 3a

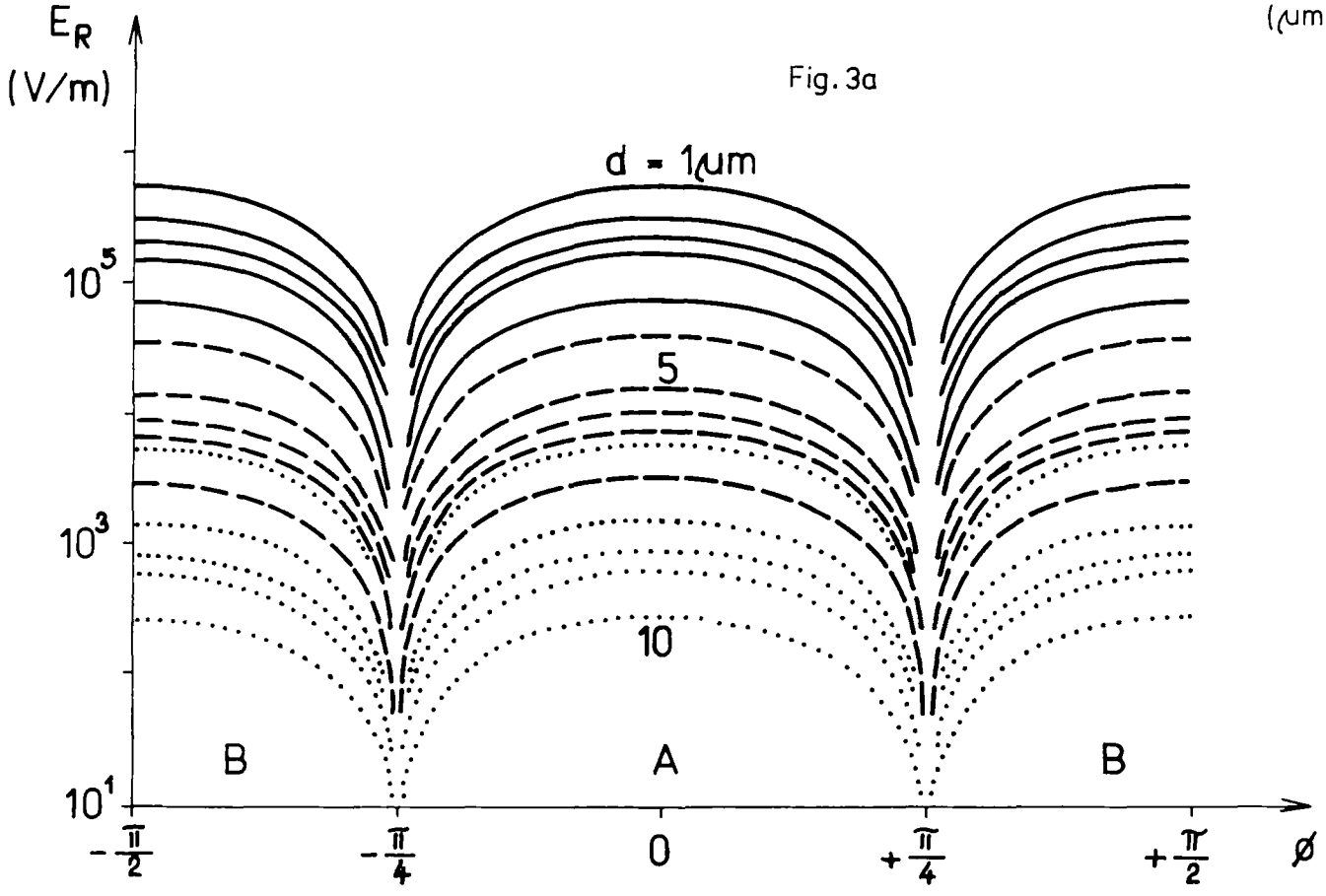


Fig. 3b

FIGURE 3

Tesseral harmonics field in the frequency range 0.1 - 10 THz (in the equatorial plane). a) The amplitude E_R of the intensity versus distance d. $\phi = 0$. b) The amplitude E_R of the intensity versus the spherical coordinate ϕ in the distance 1 (the full lines), 5 μm (the dashed lines) and 10 μm (the dotted lines). The A and B region indicate that the phase ψ of the intensity is in the range $\Pi/2 < \psi < 3\Pi/2$ and $3\Pi/2 < \psi < 2\Pi$ or $0 < \psi < \Pi/2$, respectively.

DISCUSSION

A dissipative medium is assumed to be around the cells. This leads to a more realistic picture of the field generated than the assumption of a lossless medium, especially in the frequency range under 1 GHz. Computed values of the electric field intensities for a lossless medium are greater than those for a dissipative one.

High-frequency currents flowing in conductive media create time-varying charges at the boundaries. The charge may be accumulated at or near the surface of the field-generating cell and may screen the radiation. A static charge region exists at the outer surface of the cellular membranes. The electric field intensities reach very high values in this region. A step conductivity change occurs at the interface between the membrane and the ambient medium, which is important for the screening charge accumulation.

The effect of the screening charge may be roughly assessed from the dielectric relaxation time constant τ of the liquid medium outside the cell. The time constants of water (the main component of the extracellular liquid) in the frequency range 1 GHz - 10THz are given in Table 1. τ equals approximately a quarter of the oscillation period. $\tau_f/4$ for the frequency above 0.3 THz and τ is greater than or equal to $\tau_f/4$ in the frequency range below 10 GHz. The greatest rate of the screening charge accumulation may be expected to be equal to exp(+1) and, therefore, the electromagnetic field may be built up around the cell in these frequency bands. In the frequency range 1 - 10 GHz there may occur significant screening, if the conductivity values are greater than those in Table 1 (e.g. for $\tau' = \varepsilon'\varepsilon_o/(\sigma+\sigma_o)$, σ_o = 10 S/m).

Besides the screening charge effects the resonance absorption may reduce the intensity of the electric field generated by the cell.

A large number of discrete dipoles are located in the spherical source layer. Vector sums of all the dipole contributions (with different phase, amplitude, and space orientation) determine the generated field. The field generated by the uniform as well as nonuniform dipole layers always exhibits interference lobe patterns. The lobe patterns reflect discrete source nature, inhomogeneity of the medium, and space dependence of the dipole parameters. A fine lobe pattern is connected with the discrete source nature. The fine lobe pattern is significant in the vicinity of the source layer. Extensive lobes may be generated in the case of nonuniform dipole layers. A wide variety of lobe structures may be generated by real cellular sources.

Location of vibration systems and space dependence of their parameters and of energy supply may be significant for coherent state formation and for electromagnetic field generation. The excitation level may depend on the space coordinates. Energy channeling from the vibration systems with a high energy storage to those with a low energy one may be expected. Further analysis of the space dependence of the coherent state excitation is necessary to derive an appropriate rate equation including all important space characteristics (e.g. space-dependent energy supply and channeling).

Energy consumption of a cell is increased by electromagnetic field generation. Conductivity and radiation losses occur. The smallest field intensities may be met for multipole oscillations and for dipole oscillations whose space characteristics are matched to the inner cellular inhomogeneities. An isolated cell in certain periods of its life very likely saves its energy sources by generating a weak field. Interaction with another cell or with a solid-state surface located in the proximity may modify this state.

CONCLUSION

The Fröhlich coherent vibrations are assumed to be a source of the cell-generated electromagnetic field. A spherical model of the cell in biological systems is adopted for computer simulation. Electric dipoles located at a spherical surface may generate a perceivable field within a distance of about 1 - 10 μm from the cellular surface. The computed results suggest that the intensities of the electric field may reach the values of 10^4 V/m and 10^3 V/m at the distance of 1 μm and 10 μm, respectively. The multipole layers generate considerably smaller intensities of the electric field than the dipole ones.

The computed results may be helpful in developing appropriate measuring methods. Experimental examinations are necessary to reveal the intensity, the frequency, and the space patterns of the cell-generated electromagnetic field and its changes bound to the cell cycle. The field may have several discrete spectral components. The frequency spectrum changes or the extinction of the coherent field as well as the multipole-dipole transitions and the uniform-domain oscillation transitions may reflect not only the cell cycle conditions but also the deformations and the defects of the intracellular processes (i.e. deviations from a healthy state). For example, the direct detection of the cell-generated field by a Schottky barrier or by a modified field effect transistor structure may be used.

REFERENCES

Del Giudice, E.; Doglia, S.; Milani, M. 1982. *Phys. Lett. 90A,* 104.

Fröhlich, H. 1968a. *Phys. Lett. 26A,* 402.

Fröhlich, H. 1968b. *Int. J. Quantum Chem. 2,* 641.

Fröhlich, H. 1972. *Phys. Lett. 39A,* 153.

Fröhlich, H. 1977. *Riv. Nuovo Cim. 7,* 399.

Fröhlich, H. 1978. *IEEE Trans. MTT-26,* 613.

Fröhlich, H. 1980. *Adv. Electronics Electron Phys. 53,* 85.

Fröhlich, H. 1983. *Int. J. Quantum Chem. 23,* 1589.

Pohl, H. A. 1980a. *Int. J. Quantum Chem.: Quantum Biol. Symp. 7, 18,* 411.

Pohl, H. A. 1980b. *J. Biol. Phys. 8,* 45.

Pohl, H. A.; Braden, T.; Robinson, S.; Piclardi, J.; Pohl, D. G. 1981. *J. Biol. Phys. 9,* 133.

Pokorny, J. 1980. *Czech. J. Phys. B30,* 1339.

Pokorny, J. 1982. *J. Theor. Biol. 98,* 21.

Pokorny, J.; Jandova, A.; Heyberger, K.; Kobilkova, J.; Hraba, T. 1983. *J. Theor. Biol. 102,* 295.

Rowlands, S.; Sewchand, L. S. 1982. *Can. J. Physiol. Pharmacol. 60,* 52.

Rowlands, S.; Sewchand, L. S.; Enns, E. G. 1982. *Phys. Lett. 87A,* 256.

Rowlands, S.; Sewchand, L. S.; Lovlin, R. E.; Beck, J. S.; Enns, E. G. 1981. *Phys. Lett. 82A,* 436.

Roy, S. C.; Braden, T.; Pohl, H. A. 1981. *Phys. Lett. 83A,* 142.

Sewchand, L. S.; Roberts, D.; Rowlands, S. 1982. *Cell Biophys. 4,* 253.

Stratton, J. A. 1941. *Electromagnetic Theory.* McGraw-Hill: New York-London.

Webb, S. J. 1980. *Phys. Reports 60,* 201.

Webb, S. J.; Stoneham, M. E.; Fröhlich, H. 1977. *Phys. Lett. 63A,* 407.